Electrochemistry Communications 114 (2020) 106715

Contents lists available at ScienceDirect

Electrochemistry Communications

journal homepage: www.elsevier.com/locate/elecom

Synthesis of Au@ZIF-8 nanocomposites for enhanced electrochemical detection of dopamine

Shun Lu[a,*], Matthew Hummel[a], Ke Chen[b], Yue Zhou[b], Shuai Kang[c], Zhengrong Gu[a,*]

[a] Department of Agricultural and Biosystems Engineering, South Dakota State University, Brookings, SD 57007, USA
[b] Department of Electrical Engineering and Computer Science, South Dakota State University, Brookings, SD 57007, USA
[c] Chongqing Institute of Green and Intelligent Technology, Chinese Academy of Sciences, Chongqing 400714, People's Republic of China

ARTICLE INFO

Keywords:
Au@ZIF-8
Dopamine
Electrochemical sensor
Hydrothermal method

ABSTRACT

Gold nanoparticles and zeolitic imidazolate framework-8 nanocomposites (Au@ZIF-8) were synthesized through a simple hydrothermal method and used as an enzyme-free sensor for dopamine detection. Various characterizations were used to investigate the structure and morphology of Au@ZIF-8 nanocomposites. The electrochemical performance of Au@ZIF-8 nanocomposite modified glassy carbon electrode (Au@ZIF-8/GCE) was examined in 0.1 M phosphate-buffered saline with different concentrations of dopamine. Consequently, Au@ZIF-8/GCE possessed an excellent electrochemical catalytic performance to dopamine, having been reported to its wider linear range from 0.1 to 50 μM, lower detection limit of 0.01 μM (S/N = 3) and higher sensitivity of 6.452 μA mM^{-1} cm^{-2}. The proposed sensor exhibited acceptable stability and repeatability due to the coupling effect of Au nanoparticles and ZIF-8. All the evidence suggested a potential application of Au@ZIF-8 nanocomposites in a non-enzymatic dopamine sensor.

1. Introduction

Dopamine (DA) is a well-known neurotransmitter, playing important roles in the brain and body [1,2]. However, a deficiency of DA in the human body could lead to neurological disorders, but a high level of DA could cause an increased risk of depression [3]. So, the significance of DA in the clinical diagnostic perspectives has drawn great awareness for the development of sensitive and reliable techniques for their determination [4–6]. A series of detective methods have been reported for DA determination, such as spectrophotometry, flow injection, and electrophoresis [1,7–10]. Among them, electrochemical methods have the advantages of simple instrumentation, high sensitivity and selectivity, and rapid response [1,11–14].

Zeolitic imidazolate framework-8 (ZIF-8), which is a kind of ZIFs built from Zn^{2+} ions and 2-methylimidazolate, is an attractive subclass of metal–organic frameworks (MOFs) due to the ease preparation, the great thermal, hydrothermal and chemical stabilities [15–18]. There have been increasing concerns about the application of MOFs in the electrochemical field [19–21]. However, most of the MOFs are insulators and the direct application of single MOFs in electrochemistry is limited by their poor conductivity and weak electrocatalytic abilities [17,21–23]. To address this problem, it was proposed to introduce the highly electrically conductive and electroactive materials into MOFs, further improving the sensitivity of the modified electrode. Metal nanoparticles decorated MOF compounds exhibit significantly enhanced performance including high electrical conductivity and outstanding electrocatalytic activity [24–26]. These features have led to the increasing use of MOFs/metal nanoparticle (NP) composites in the fabrication of electrochemical biosensors [27–29]. Among the more commonly used metal NPs, gold (Au) is the most widely studied. Au NPs have been broadly reported for their high catalytic activity which could facilitate the electron transfer rate [30].

Herein, Au@ZIF-8 nanocomposites were successfully fabricated and modified on glassy carbon electrode (GCE) for electrochemical determination of dopamine. The as-prepared nanocomposites show high sensitivity, low LOD (limit of detection), good selectivity, reproducibility and stability for the determination of DA due to the synergistic effect of Au NPs and ZIF-8 with larger surface area. It is expected to be applied in practical DA detection.

2. Experimental section

2.1. Materials.

Gold (III) chloride hydrate ($HAuCl_4$, AR), sodium borohydride ($NaBH_4$, AR), polyvinyl pyrrolidone (PVP, M = 20000), zinc nitrate

* Corresponding authors.
E-mail addresses: Shun.Lu@sdstate.edu (S. Lu), Zhengrong.Gu@sdstate.edu (Z. Gu).

https://doi.org/10.1016/j.elecom.2020.106715
Received 20 February 2020; Received in revised form 18 March 2020; Accepted 19 March 2020
Available online 21 March 2020

hexahydrate ($Zn(NO_3)_2$ $6H_2O$, 98%), 2-methyimidazole (abbreviated to 2-MeIm) were purchased from Fisher Scientific™ and Sigma-Aldrich™ in USA. Methanol and ethanol were both used with AR grade. The phosphate buffer solution (PBS, 0.1 M was prepared by mixing Na_2HPO_4 and NaH_2PO_4 stock solution and adjusted pH value with 0. 1 M H_3PO_4 or NaOH, which was used as the supporting electrolyte during the whole process. Ultrapure water (18.5 MΩ, made in Lab) was used throughout the whole experiment.

3. Synthesis of Au@ZIF-8 nanocomposites

Au@ZIF-8 NPs were synthesized using the solvothermal method with minor revision [15,23]. Briefly, the gold nanoparticle (Au NP) solution was prepared by the reduction of $HAuCl_4$ (39.1 mg) with $NaBH_4$ (38 mg) with the protection of PVP (111 mg). Then, the PVP-stabilized Au NPs were collected by centrifugation and washed three times with ethanol solution after vigorous stirring (30 min). Furthermore, the synthesized Au NP solution (2 mL, 1 mg mL^{-1}) mixed with 2-MeIm (15 mL, 50 mM) in methanol. Afterward, $Zn(NO_3)_2$ $6H_2O$ (15 mL, 50 mM) in methanol was added quickly. The mixed solution was sonicated for 30 min. Subsequently, the violet precipitate was collected by centrifugation and washed three times with ethanol, then dried under vacuum at 60 °C for 4 h to yield a dark red powder (named Au@ZIF-8 nanocomposites). Additionally, ZIF-8 NPs were prepared with the same procedures as a comparison.

4. Fabrication of Au@ZIF-8 nanocomposites modified GCE

For fabrication of electrode, Au@ZIF-8 nanocomposites (1.5 mg) were ultrasonically dispersed in ethanol (1.5 mL) for ~30 min, as shown in Scheme 1. Before modification, the glassy carbon electrode (GCE, 4 mm in diameter) was polished sequentially with 5.0 μm, 0.5 μm Al_2O_3 powder and then washed ultrasonically in distilled water before each experiment. Then, a drop of the suspension (4.0 μL, 1.0 mg mL^{-1}) was covered on the surface of polished GCE, then cast with Nafion (wt. 5.0%, 4.0 μL) and dried in an inverted beaker at room temperature. The loading catalyst on the GCE is ~0.08 mg cm^{-2}.

5. Physical characterization

The morphology and crystalline information were characterized by Scanning electron microscopy (SEM, FEI Siri200), energy dispersive X-ray spectroscopy (EDX), X-ray diffraction (XRD, Rigaku-SmartLab) and transmission electron microscopy (TEM, JEM-2100, Japan) equipped with STEM-EDX. Nitrogen adsorption–desorption isotherms were measured with a Micrometrics instrument (ASAP 2020, USA) at 77 K.

6. Electrochemical measurements

The electrochemical measurements were performed by cyclic voltammetry (CV), electrochemical impedance spectroscopy (EIS), differential pulse voltammetry (DPV) and amperometric *i-t* using a potentiostat (CHI 760e, USA) with equipped software. The electrochemical tests were conducted at room temperature using the three-electrode setting in 0.1 M PBS as an electrolyte. Here, Ag/AgCl (saturated KCl solution) and platinum wire were used as a reference electrode and a counter electrode, Au@ZIF-8 and ZIF-8 were modified on glassy carbon electrodes (GCE) using as working electrode, respectively.

7. Results and discussion

The morphologies and structures of the as-prepared nanomaterials were presented in Fig. 1. Fig. 1A clearly displays that these nanoparticles are found to be monodisperse, polyhedral in shape with an average size of 270 ± 10 nm. And all the peaks observed in the XRD keep consistency with the simulated result of ZIF-8 (Fig. 1B) [23]. Fig. 1C shows a typical TEM image of Au@ZIF-8 nanocomposites, and the presence of well-distributed Au on ZIF-8 NPs was confirmed by STEM-EDX mapping (Fig. 1E) which shows uniform distribution of Au on ZIF-8 NPs. The ZIF-8 provided more surface area for Au NPs (black dots in Fig. 1C) and Au NPs in the edge were dispersed on the surface of the as-prepared nanocomposites. The synergistic effect of between the selectivity of Au NPs and the large surface of ZIF-8 NPs could enhance the analytical performance of this electrochemical sensor. Combined with the above characterizations, it implies that the Au@ZIF-8 nanocomposites were successfully synthesized.

Nitrogen adsorption–desorption isotherms of Au@ZIF-8 nanocomposites and pore size distribution are shown in Fig. 2. The N_2 adsorption of Au@ZIF-8 nanocomposites exhibited type I profile, which indicated that Au@ZIF-8 nanocomposites were dominated by microporous structure, as presented in Fig. 2A. The surface area of Au@ZIF-8 nanocomposites is 1594 m^2 g^{-1}, and a microporous volume of 0.65 cm^3 g^{-1}, which is a little higher than the pure ZIF-8 nanoparticles' surface area [23,31]. This is due to the introduction of Au NPs on the surface of ZIF-8, further increase the surface area of the as-obtained materials [31]. The increase in the volume adsorbed at very low relative pressures is owing to the existence of microspores. The pore size distribution calculated using the DFT method showed that Au@ZIF-8 nanocomposites were composed of the uniform pore with a narrow distribution (Fig. 2B). The above-analyzed results implied that increased specific surface area and unique porous nanostructure of Au@ZIF-8 nanocomposites may provide more active sites or structure for the adsorption of DA on the larger surface, which will contribute to

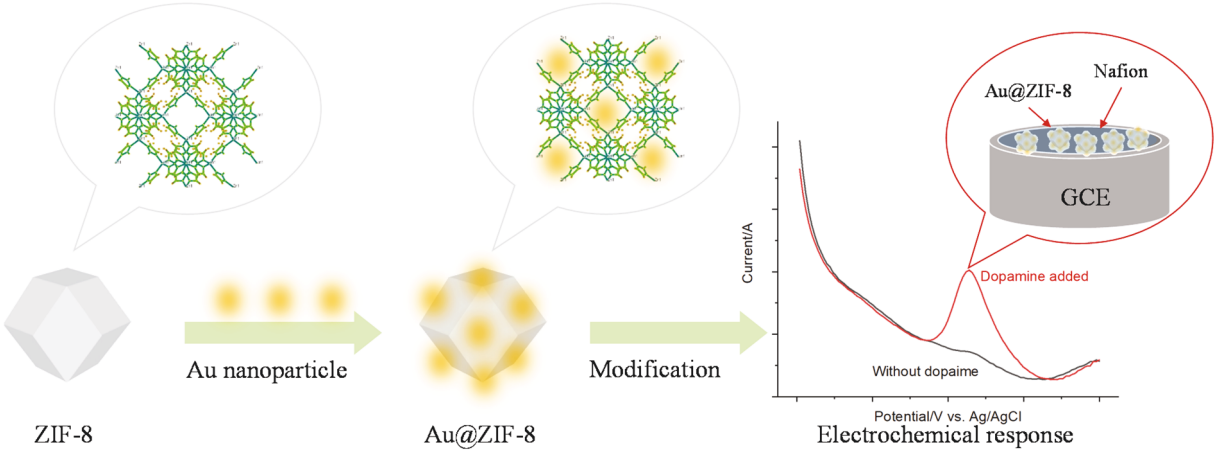

Scheme 1. Illustration of synthesis of Au@ZIF-8 nanocomposite and its electrochemical response toward dopamine.

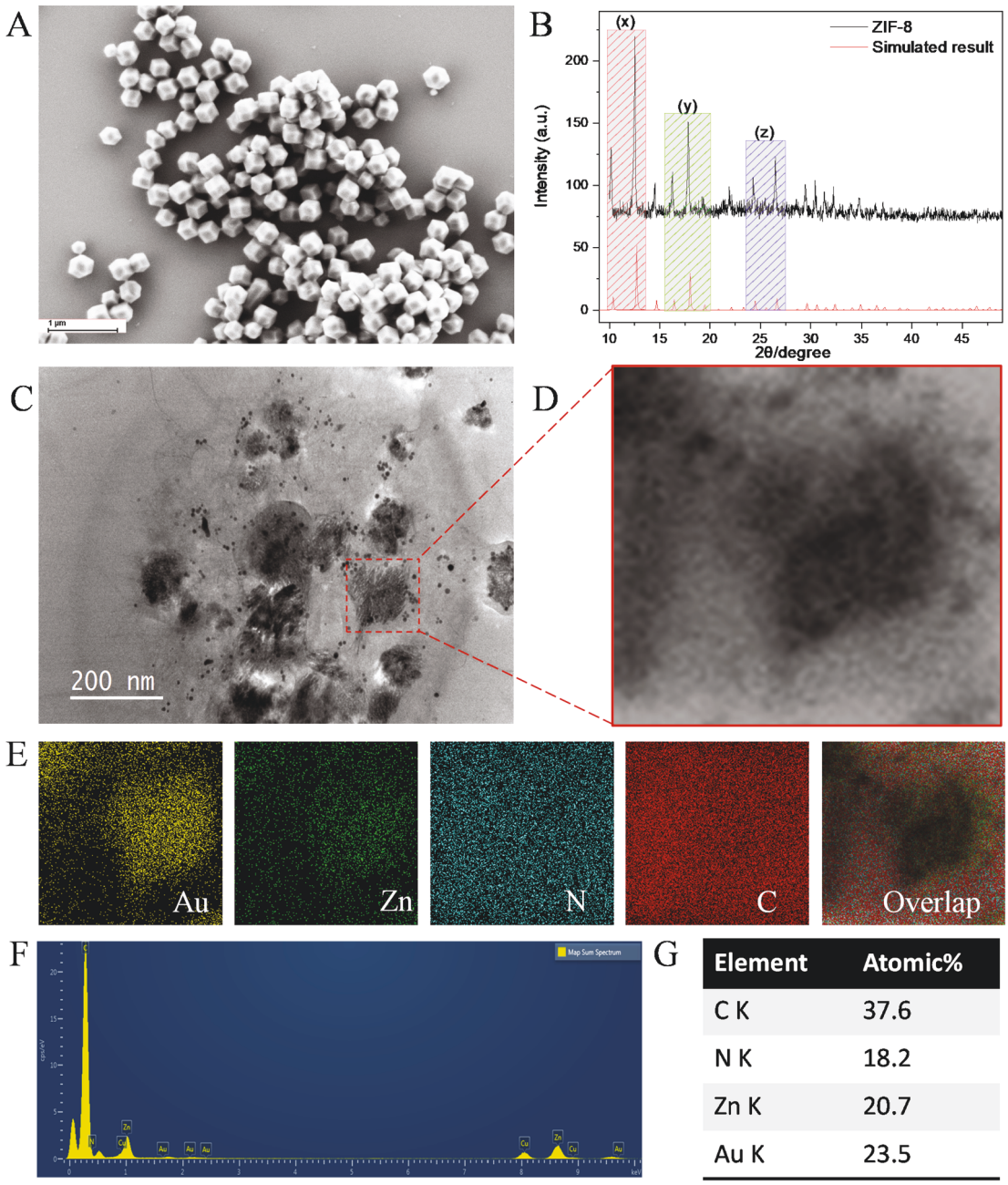

Fig. 1. (A) SEM image of ZIF-8 NPs, and (B) XRD pattern of ZIF-8 NPs, simulated result from Mercury v3.10.3; (C) TEM image of Au@ZIF-8 nanocomposites, (D) enlarged area from (C), (E) STEM-EDX mapping (Yellow for Au, Green for Zn, Cyan for N, Red for C element) of Au@ZIF-8 nanocomposites, (F) EDX spectrum with detailed table (G). (For interpretation of the references to colour in this figure legend, the reader is referred to the web version of this article.)

improving the electrocatalytic performance of the modified electrode [1,26].

Electrochemical detection of DA using the Au@ZIF-8/GCE was evaluated by electrochemical measurements. Cyclic voltammogram (CV) was employed to study the electrochemical redox of DA at the different modified electrodes. The electrochemical behavior of two modified electrodes (Au@ZIF-8/GCE and ZIF-8/GCE) in 0.1 M PBS (pH = 7.0) solution in the absence and presence of 0.5 mM DA was examined using CV from the potential range from −0.2 to 0.6 V (*vs.* Ag/AgCl), as shown in Fig. 3A. The Au@ZIF-8/GCE exhibits a larger peak current compared to the oxidation current obtained at the ZIF-8/GCE. It indicated that Au@ZIF-8/GCE has a larger relatively electrochemical surface area. The stepwise fabrication of the electrochemical sensor was also characterized by using CV (Fig. 3B). The ZIF-8/GCE showed a pair of reduction and oxidation peaks in 1.0 mM $[Fe(CN)_6]^{3-/4-}$ containing 0.1 M KCl (black line in Fig. 3B) with *ca.* area of 1.741×10^{-5} (calculated from the given closed curve). After the introduction of Au NPs, a larger pair of redox peaks were appeared (red line in Fig. 3B) with *ca.* area of 2.104×10^{-5}, further confirmed its better charge transferability due to the presence of Au NPs. The effect of pH value of the detecting electrolyte on the electrooxidation of DA was investigated. As shown in Fig. 3C, the oxidation peak current of DA increased with increasing pH value from 6.2 to 7.4, and decreased from 7.4 to 8.0, therefore, pH 7.6 in 0.1 M PBS was selected as the optimal experimental condition.

Fig. 3D depicts the linear dependence of the reduction/oxidation peak currents on the square root of the scan rate, which confirming that the oxidation of DA is a typical diffusion-controlled process. Tafel slopes (Fig. S1) of Au@ZIF-8/GCE and ZIF-8/GCE were obtained from linear sweep voltammetry (LSV, Fig. 3E), suggesting Au@ZIF-8/GCE

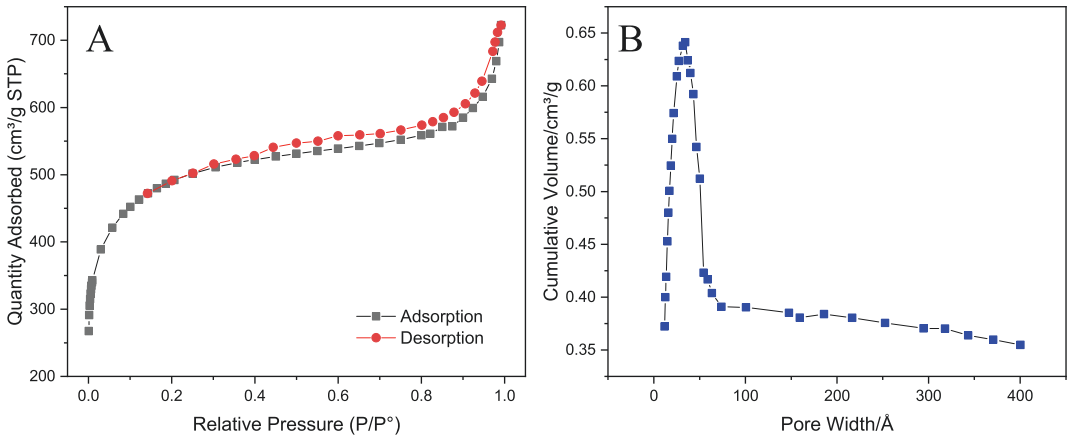

Fig. 2. Nitrogen adsorption and desorption isotherm (A) and the corresponding pore size distribution curve (B) of Au@ZIF-8 nanocomposites.

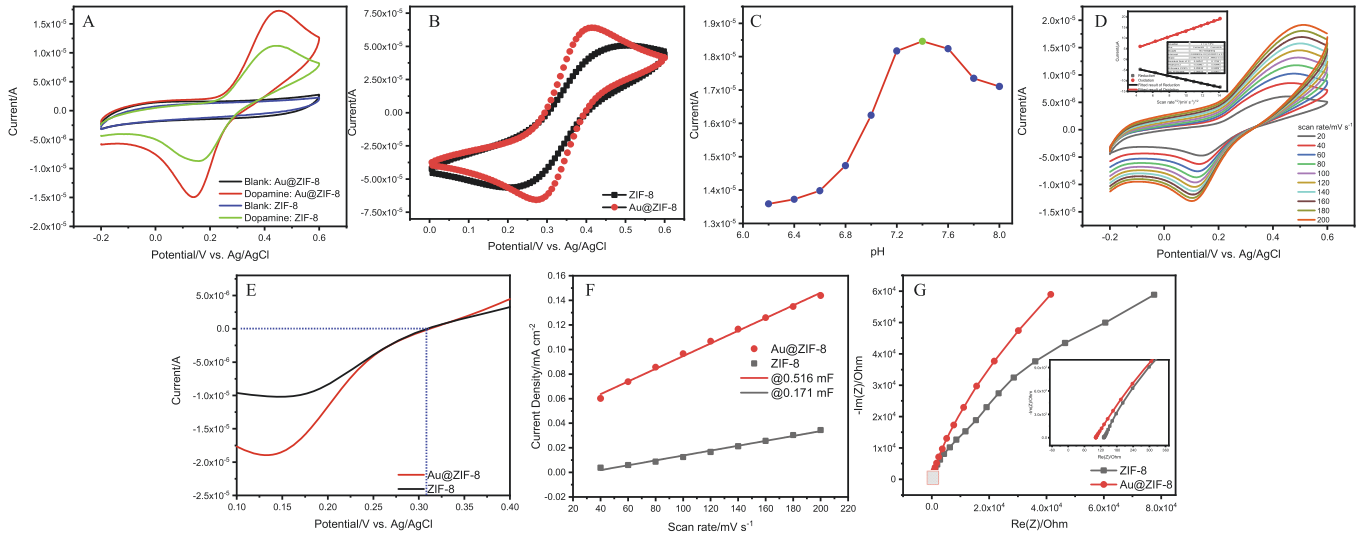

Fig. 3. (A) CVs on the Au@ZIF-8/GCE and ZIF-8 in 0.1 M PBS (pH 7.0) with 0.5 mM DA, scan rate: 50 mV s^{-1}, (B) CVs at Au@ZIF-8/GCE and ZIF-8/GCE in 1.0 mM $[Fe(CN)_6]^{3-/4-}$ solution containing 0.1 M KCl, scan rate: 50 mV s^{-1}. (C) The effect of pH on the current response of 0.5 μM DA at Au@ZIF-8/GCE, (D) CVs of Au@ZIF-8 in 0.1 M PBS containing 0.5 μM DA at different scan rates from 20 to 200 mV s^{-1}, inset: the linear dependence of the reduction peak current and oxidation peak current on the square root of the scan rate. (E) LSV plots of Au@ZIF-8 and ZIF-8 electrodes in 0.1 M PBS (pH 7.4) with 0.5 mM DA. (F) Plots of the averaged current density at −0.1 V against scan rates. (G) Nyquist plots of ZIF-8/GCE and Au@ZIF-8/GCE in the presence of 0.1 M PBS solution (pH 7.4).

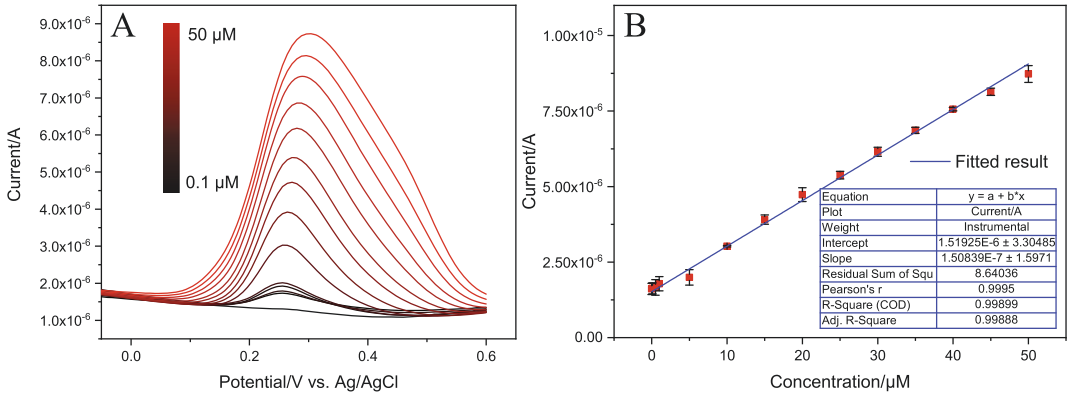

Fig. 4. (A) DPV of DA with increasing concentration (from black to red: 0.1 to 50 μM), (B) The relationship of the oxidation peak current (*Ipa*) with the concentration of DA. (For interpretation of the references to colour in this figure legend, the reader is referred to the web version of this article.)

performed better electrochemical kinetics than that of ZIF-8/GCE [13,32]. The electrochemical double-layer capacitances (C_{dl}) of Au@ZIF-8 is 3 times higher than that of ZIF-8, further confirming its larger active surface areas in the Fig. 3F [33]. EIS is an effective tool for probing the interfacial behavior of modified electrodes. Fig. 3G shows that the Nyquist plots of Au@ZIF-8/GCE and ZIF-8/GCE, it is observed that the Nyquist plot of Au@ZIF-8/GCE is almost linear, while that of ZIF-8/GCE with the similar trend which consists of a quasi-semicircular

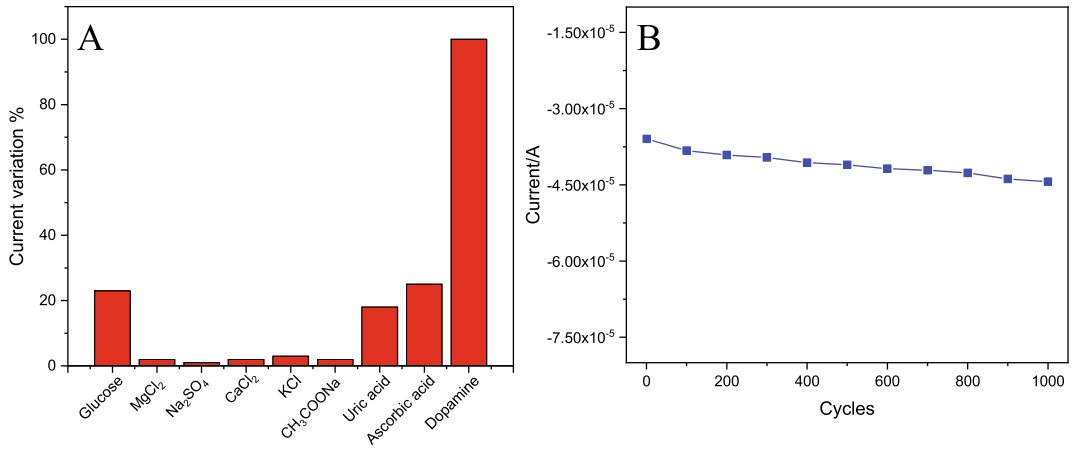

Fig. 5. (A) The signal enhancement of current in the presence of diverse kinds of interfering substance, respectively. (B) The peak currents collected after 1000-cycle CVs run in 0.1 M PBS (pH 7.4) solution containing 5.0 mM DA.

arch at high frequencies and an oblique line at low frequencies. It implies that Au@ZIF-8/GCE acts as a better conducting material and accelerates the electron transfer process at the electrode surface [23]. Consequently, it concluded that the presence of Au NPs, and larger electrochemical surface area and low electrochemical resistance, which synergistic facilitate the oxidation of DA.

The performance of the as-prepared electrochemical sensor was investigated by the DPV measurements using the Au@ZIF-8/GCE in 0.1 M PBS (pH 7.4) upon the successive addition of different concentrations of DA solutions, as shown in Fig. 4A. The electrolyte was stirred for ~10 s to confirm that the added DA was fully mixed in the electrolyte. The peak at around 0.25 V appeared with the addition of DA. And the peak current gradually increased and was proportional to the DA concentrations with a wide linear range from 0.1 to 50 μM with the correlation coefficient of 0.998 (Fig. 4B). The sensitivity of Au@ZIF-8/GCE is calculated to be 6.452 $\mu A\ mM^{-1}\ cm^{-2}$ in the detected concentration range. The proposed Au@ZIF-8/GCE has a larger concentration range than ZIF-8/GCE (Table S1). Furthermore, the estimated value of LOD (limit of detection) is approximately 0.01 μM (S/N = 3). This may be due to the high conductivity which is essential to the enhancement of electrocatalytic to the detection of DA [34]. It can be found that Au@ZIF-8/GCE exhibited a broader detection range and lower LOD, which had better sensitivity for the DA detection.

The selectivity of Au@ZIF-8/GCE is studied by detecting DA in the presence of several inorganic salts, glucose (Glu), uric acid (UA), and ascorbic acid (AA). As shown in Fig. 5A, the addition of inorganic salts, Glu, AA, and UA represented negligible current response compared with DA, suggesting Au@ZIF-8/GCE has an excellent selectivity to DA. The stability and repeatability of the proposed sensor was also studied. The stability of Au@ZIF-8/GCE was verified after successive 1000-cycle CVs. The oxidation peak current of DA decreased by 18% after 1000 CV cycle, as shown in Fig. 5B, indicating that good stability and reproducibility can be obtained for electrochemical detection by Au@ZIF-8/GCE. Three paralleled modified-electrodes were prepared with the same condition for evaluating the reproducibility of Au@ZIF-8/GCE by detecting current signal in 0.1 M PBS (pH 7.4) solution with successive addition of 10 μM DA and 0.5 μM urine. The relative standard deviation (RSD) of the electrodes are distributed from 0.9% to 3.3%, as displayed in Table S2, indicating that Au@ZIF-8 modified electrode is indeed reliable in practical applications.

8. Conclusions

In summary, Au@ZIF-8 nanocomposites were successfully fabricated and modified on glassy carbon electrode (GCE) for electrochemical determination of dopamine. The proposed Au@ZIF-8/GCE exhibits better sensitivity than ZIF-8/GCE, it also shows good selectivity and long-term stability. Such selectivity and comparable performance can be attributed to the synergetic electrochemical performance between Au nanoparticles and ZIF-8, and fast charge transferability between the electrochemical sites and the electrode. Therefore, Au@ZIF-8/GCE presents promising performance as a potential non-enzymatic dopamine sensor.

CRediT authorship contribution statement

Shun Lu: Conceptualization, Methodology, Software, Writing - original draft. **Matthew Hummel:** Data curation. **Ke Chen:** Visualization, Investigation. **Yue Zhou:** Supervision. **Shuai Kang:** Software, Validation. **Zhengrong Gu:** Writing - review & editing, Funding acquisition.

Acknowledgements

This work was supported by NSF/EPSCoR (No. OIA-1849206). S. Lu also acknowledges the financial support from the China Scholarship Council (CSC). Here, we pay tribute to all doctors and nurses who defend against COVID-19.

Appendix A. Supplementary data

Supplementary data to this article can be found online at https://doi.org/10.1016/j.elecom.2020.106715.

References

[1] N. Tukimin, J. Abdullah, Y. Sulaiman, Review-Electrochemical detection of uric acid, dopamine and ascorbic acid, J. Electrochem. Soc. 165 (2018) B258–B267.
[2] S. Lammel, E.E. Steinberg, C. Foldy, N.R. Wall, K. Beier, L. Luo, R.C. Malenka, Diversity of transgenic mouse models for selective targeting of midbrain dopamine neurons, Neuron 85 (2015) 429–438.
[3] D.L. Robinson, B.J. Venton, M.L. Heien, R.M. Wightman, Detecting subsecond dopamine release with fast-scan cyclic voltammetry in vivo, Clin. Chem. 49 (2003) 1763–1773.
[4] P. Seeman, Parkinson's disease treatment may cause impulse-control disorder via dopamine D3 receptors, Synapse 69 (2015) 183–189.
[5] F.T. Patrice, L.J. Zhao, E.K. Fodjo, D.W. Li, K.P. Qiu, Y.T. Long, Highly sensitive and selective electrochemical detection of dopamine using hybrid bilayer membranes, Chemelectrochem 6 (2019) 634–637.
[6] R.P. Bacil, L. Chen, S.H.P. Serrano, R.G. Compton, Dopamine oxidation at gold electrodes: mechanism and kinetics near neutral pH, PCCP 22 (2020) 607–614.
[7] J. Yu, L. Ge, J. Huang, S. Wang, S. Ge, Microfluidic paper-based chemiluminescence biosensor for simultaneous determination of glucose and uric acid, Lab Chip 11 (2011) 1286–1291.
[8] H.Y. Wang, Q.S. Hui, L.X. Xu, J.G. Jiang, Y. Sun, Fluorimetric determination of dopamine in pharmaceutical products and urine using ethylene diamine as the fluorigenic reagent, Anal. Chim. Acta 497 (2003) 93–99.

[9] M. Satyanarayana, K.K. Reddy, K.V. Gobi, Nanobiocomposite based electrochemical sensor for sensitive determination of serotonin in presence of dopamine, ascorbic acid and uric acid in vitro, Electroanalysis 26 (2014) 2365–2372.
[10] S. Lu, M. Hummel, S. Kang, Z. Gu, Selective voltammetric determination of nitrite using cobalt phthalocyanine modified on multiwalled carbon nanotubes, J. Electrochem. Soc. 167 (2020) 046515.
[11] H.Y. Yue, P.F. Wu, S. Huang, Z.Z. Wang, X. Gao, S.S. Song, W.Q. Wang, H.J. Zhang, X.R. Guo, Golf ball-like MoS_2 nanosheet arrays anchored onto carbon nanofibers for electrochemical detection of dopamine, Microchim. Acta 186 (2019) 378.
[12] M. Sajid, N. Baig, K. Alhooshani, Chemically modified electrodes for electrochemical detection of dopamine: Challenges and opportunities, Trac-Trend Anal Chem 118 (2019) 368–385.
[13] R.G. Compton, C.E. Banks, Understanding voltammetry, World Scientific, London, U.K., 2011.
[14] S.B. Hočevar, J. Wang, R.P. Deo, M. Musameh, B. Ogorevc, Carbon nanotube modified microelectrode for enhanced voltammetric detection of dopamine in the presence of ascorbate, Electroanalysis 17 (2005) 417–422.
[15] L. Chen, Y. Peng, H. Wang, Z. Gu, C. Duan, Synthesis of Au@ZIF-8 single- or multi-core-shell structures for photocatalysis, Chem. Commun. 50 (2014) 8651–8654.
[16] Y. Pan, Y. Liu, G. Zeng, L. Zhao, Z. Lai, Rapid synthesis of zeolitic imidazolate framework-8 (ZIF-8) nanocrystals in an aqueous system, Chem. Commun. 47 (2011) 2071–2073.
[17] Q.L. Song, S.K. Nataraj, M.V. Roussenova, J.C. Tan, D.J. Hughes, W. Li, P. Bourgoin, M.A. Alam, A.K. Cheetham, S.A. Al-Muhtaseb, E. Sivaniah, Zeolitic imidazolate framework (ZIF-8) based polymer nanocomposite membranes for gas separation, Energy Environ. Sci. 5 (2012) 8359–8369.
[18] B. Assfour, S. Leoni, G. Seifert, Hydrogen adsorption sites in zeolite imidazolate frameworks ZIF-8 and ZIF-11, J. Phys. Chem. C 114 (2010) 13381–13384.
[19] M. Nie, S. Lu, Q. Li, X. Liu, S. Du, Facile solvothermal synthesis of HKUST-1 as electrocatalyst for hydrogen evolution reaction, SCIENTIA SINICA Chimica 46 (2016) 357–364.
[20] C. Duan, J. Zheng, Bimetallic MOF-based enzyme-free sensor for highly sensitive and delective detection of dopamine, J. Electrochem. Soc. 166 (2019) B942–B947.
[21] M. Saraf, R. Rajak, S.M. Mobin, A fascinating multitasking Cu-MOF/rGO hybrid for high performance supercapacitors and highly sensitive and selective electrochemical nitrite sensors, J. Mater. Chem. A 4 (2016) 16432–16445.
[22] C.Y. Zhang, M.Y. Wang, L. Liu, X.J. Yang, X.Y. Xu, Electrochemical investigation of a new Cu-MOF and its electrocatalytic activity towards H_2O_2 oxidation in alkaline solution, Electrochem. Commun. 33 (2013) 131–134.
[23] M. Nie, S. Lu, D. Lei, C. Yang, Z.Z. Zhao, Rapid synthesis of ZIF-8 nanocrystals for electrochemical detection of dopamine, J. Electrochem. Soc. 164 (2017) H952–H957.
[24] A.M. Yu, Z.J. Liang, J. Cho, F. Caruso, Nanostructured electrochemical sensor based on dense gold nanoparticle films, Nano Lett. 3 (2003) 1203–1207.
[25] H. Wang, S. Zhang, S. Li, J. Qu, Electrochemical sensor based on palladium-reduced graphene oxide modified with gold nanoparticles for simultaneous determination of acetaminophen and 4-aminophenol, Talanta 178 (2018) 188–194.
[26] N.R. Devi, M. Sasidharan, A.K. Sundramoorthy, Gold nanoparticles-thiol-functionalized reduced graphene oxide coated electrochemical sensor system for selective detection of mercury Ion, J. Electrochem. Soc. 165 (2018) B3046–B3053.
[27] D.K. Yadav, V. Ganesan, P.K. Sonkar, R. Gupta, P.K. Rastogi, Electrochemical investigation of gold nanoparticles incorporated zinc based metal-organic framework for selective recognition of nitrite and nitrobenzene, Electrochim. Acta 200 (2016) 276–282.
[28] J.C. Jin, J. Wu, G.P. Yang, Y.L. Wu, Y.Y. Wang, A microporous anionic metal-organic framework for a highly selective and sensitive electrochemical sensor of Cu^{2+} ions, Chem. Commun. 52 (2016) 8475–8478.
[29] C.-L. Sun, H.-H. Lee, J.-M. Yang, C.-C. Wu, The simultaneous electrochemical detection of ascorbic acid, dopamine, and uric acid using graphene/size-selected Pt nanocomposites, Biosens. Bioelectron. 26 (2011) 3450–3455.
[30] L. Wang, T. Meng, Y. Fan, C. Chen, Z. Guo, H. Wang, Y. Zhang, Electrochemical study of acetaminophen oxidation by gold nanoparticles supported on a leaf-like zeolitic imidazolate framework, J. Colloid Interface Sci. 524 (2018) 1–7.
[31] L. Cheng, Y.J. Fan, X.C. Shen, H. Liang, Highly sensitive detection of dopamine at ionic liquid functionalized RGO/ZIF-8 nanocomposite-modified electrode, Journal of Nanomaterials (2019) 8936095.
[32] D. Li, C. Lin, C. Batchelor-McAuley, L. Chen, R.G. Compton, Tafel analysis in practice, J. Electroanal. Chem. 826 (2018) 117–124.
[33] S. Lu, M. Hummel, Z. Gu, Y. Gu, Z. Cen, L. Wei, Y. Zhou, C. Zhang, C. Yang, Trash to treasure: A novel chemical route to synthesis of NiO/C for hydrogen production, Int. J. Hydrogen Energy 44 (2019) 16144–16153.
[34] G. Zhu, Z. He, J. Chen, J. Zhao, X. Feng, Y. Ma, Q. Fan, L. Wang, W. Huang, Highly conductive three-dimensional MnO_2-carbon nanotube-graphene-Ni hybrid foam as a binder-free supercapacitor electrode, Nanoscale 6 (2014) 1079–1085.